Eur J Vasc Endovasc Surg (2019) 58, 538–547

Endograft Specific Haemodynamics After Endovascular Aneurysm Repair: Flow Characteristics of Four Stent Graft Systems

Anastasios Raptis [a], **Michalis Xenos** [a,b], **Konstantinos Spanos** [c], **George Kouvelos** [c], **Athanasios Giannoukas** [a,c], **Miltiadis Matsagkas** [a,c,*]

[a] Laboratory for Vascular Simulations, Institute of Vascular Diseases, Larissa, Greece
[b] Department of Mathematics, University of Ioannina, Ioannina, Greece
[c] Department of Vascular Surgery, Faculty of Medicine, School of Health Sciences, University of Thessaly, Larissa, Greece

WHAT THIS PAPER ADDS

Deployment of an endograft, in the context of endovascular aneurysm repair, alters blood flow conditions potentially to the point where an adverse event is likely. Through computational simulations, it is possible to gain access to high resolution haemodynamic indices. This study relies on computational fluid dynamics to deal with blood flow variability among four stent graft systems, seeking unique haemodynamic characteristics. For the first time, several endografts are studied in parallel. To increase the level of endovascular treatment personalisation and further improve endograft design, it is important initially to define and evaluate the haemodynamic characteristics of existing devices.

Objectives: The implication of haemodynamics in the occurrence of complications after endovascular aneurysm repair (EVAR) has been raised in the literature. Different aortic stent graft configurations may lead to different haemodynamic properties. The current study deals with the post-operative haemodynamic variability between four stent graft systems with different structure, material, and type of fixation.

Methods: Computed tomography data of 32 patients were used, equally distributed among the four endograft groups, namely the AFX, Endurant, Excluder, and Nellix. Velocity, wall shear stress (WSS), and helicity statistics were calculated, in regions around the flow division where disturbances are expected. The haemodynamic data were compared between and within the groups.

Results: The morphology of AAAs pre-operatively did not vary significantly among the four groups. Before the flow division, lowest velocity was observed in Endurant cases and highest in Nellix cases. Endurant induced the lowest peak WSS and Nellix the highest ($p = .03$). The helicity levels were low in AFX and Nellix cases and high in Endurant and Excluder cases. After the flow division, the trend in the results was preserved. Nellix induced the highest velocity and WSS, followed closely by Excluder and AFX. There was a significant increase of helicity before and after flow division in AFX ($p < 0.001$, $R^2 = 0.09$) and Nellix ($p < 0.001$) cases.

Conclusions: It has been shown that different types of endografts induce variable haemodynamic conditions around the flow division. The parallel limb structure, featured by Nellix, seems to induce favourable flow conditions in terms of velocity and WSS, while helical flow before the flow division is suppressed. High WSS is generally considered to be a desirable flow characteristic in endovascular devices, whereas helicity extremes (very low or high) are potentially a negative sign. Endurant, with the stiffer material and the short neck structure, was associated with the lowest blood velocity and WSS values but preserved high helicity levels. The AFX and Excluder, which include the same material, induced similar haemodynamic conditions.

Keywords: Computational fluid dynamics, Endovascular aneurysm repair, Endograft specific simulations, Haemodynamic variability, Stent graft
Article history: Received 5 April 2018, Accepted 14 April 2019, Available online 17 August 2019

INTRODUCTION

During the last two decades, endovascular aneurysm repair (EVAR) has emerged as the treatment of choice for the management of elective and ruptured abdominal aortic aneurysms (AAAs).[1–3] There have been four eras in the development of EVAR: physician made grafts; early industry devices; intermediate commercial endografts; and modern stent grafts. The evolution of EVAR has brought

* Corresponding author. General University Hospital of Larissa, Mezourlo 41110, Larissa, Greece.
E-mail addresses: mimats@med.uth.gr; milmats@gmail.com (Miltiadis Matsagkas).
1078-5884/
https://doi.org/10.1016/j.ejvs.2019.04.017

improvements in efficiency, outcomes, and procedural success.[4] However, re-intervention has been shown to be more common in EVAR than open repair.[5]

The interdisciplinary approach combining the clinical and mechanical aspects behind the placement of an endovascular device has boosted research on outcomes after EVAR. An endovascular device can successfully reduce sac pressure, mechanical stress, and pulsatile wall motion,[6] while increased drag forces as a result of blood pressure acting on the device were also detected.[7] The recently introduced endovascular sealing technology (EVAS), featured in the Nellix device, was studied by Argani et al.,[8] showing that static forces and vibrations during daily activities can disturb an EVAS device. A computational mechanics analysis can assist in evaluating the likelihood of post-EVAR aneurysm shrinkage.[7]

Computational fluid dynamics (CFD) simulations are widely used in the research for the haemodynamic impact of endograft placement.[9,10] The post-EVAR morphology of the lumen determined by the stent graft system could favour regions in which disturbed haemodynamics are developing. The development of thrombus, immediately after the implantation or after months,[11] can be triggered in regions where low wall shear stresses (WSS) prevail.[12] Study of thrombosis in endografts is high in the research priorities according to the Vascular Surgery Society practice guidelines on the care of AAA patients.[13] Early post-operative intra-prosthetic thrombus development has also been connected with widespread blood recirculation.[14–17] Virchow was the first to recognise that blood flow plays an important role in thrombosis.[18]

In-stent haemodynamics is the main methodology in studies focusing on endograft designs that can minimise stent graft failure.[19–22] Casciaro et al.[23] found that AFX and Nellix decrease the reflected wave transient time, while Nellix shows increased reflected wave amplitude at the proximal abdominal aorta and at renal artery level compared with AFX. A CFD evaluation of the Ovation stent graft device, which accommodates challenging anatomies using inflatable O rings, is provided by Aristokleous et al.[24] Their study highlighted high shear rate and strong recirculation zones developing near the stenotic region, which could lead to a functional impact on the device under exercise flow conditions. Accordingly, the present study group has performed haemodynamic evaluation of various endografts accounting for the haemodynamic variability among patients and endografts. It was shown that AFX, which achieves fixation by using the aortic bifurcation, restores blood flow at physiological levels with respect to the studied haemodynamic indices, while Nellix was equivalently efficient with emphasis on the observed suppression of helical flow at the entrance to the device.[25] Studying two widely used devices with similar structure but different material, it was found that Endurant and Excluder induced different haemodynamic conditions post-operatively.[26,27] More recently, an extended analysis of these two devices revealed sites on the implanted endovascular device that might be favourable to thrombus formation initiation and the value of morphometry as a tool to predict haemodynamic features was also highlighted.[28] The significance of the endograft position post-operatively, as a factor that potentially promotes the emergence of post-operative complications, is also acknowledged by Perrin et al.,[29] who developed a computational framework for EVAR planning.

The current study deals with the post-EVAR CFD in four stent graft systems with different designs, materials, and types of fixation (Table 1). Specifically, the endovascular devices under consideration were: the AFX (Endologix, Irvine, CA, USA); Endurant (Medtronic, Minneapolis, MN, USA); Excluder (Gore, Newark, DE, USA); and Nellix (Endologix, Irvine, CA, USA). An endograft specific approach was applied, analysing flow statistics based on a sample of patients in each endograft group. Through CFD simulations, the post-operative flow field was acquired and attention was drawn to the properties of blood flow in the zones surrounding the endograft bifurcation. The haemodynamic properties (velocity, WSS, and helicity) were compared statistically among the devices, to test whether the endografts under consideration have unique haemodynamic characteristics.

METHODS

Materials

The cases considered suitable for the study were exclusively EVAR treated patients with fusiform AAAs not extending to common iliac arteries. In total, medical imaging data of 32 cases were used, equally distributed among the four endograft groups according to their instructions for use (IFU). Specifically, the data came from computed tomography (CT) scans performed pre-operatively and one month

Table 1. Endografts under consideration with their specifications regarding graft and stent material, and fixation methods

	Stent	Graft	Fixation
AFX	Cobalt chromium	Expanded polytetrafluoroethylene (ePTFE)	Suprarenal/aortic bifurcation
Endurant	Nitinol	Polyester fabric	Suprarenal/proximal anchoring pins
Excluder	Nitinol	ePTFE and fluorinated ethylene polypropylene	Proximal nitinol barbs
Nellix	Cobalt chromium	PTFE	Endobags filled with polyethylene glycol

Table 2. Basic size characteristics of the stent graft systems placed in each case

Patient	Main body diameter, mm	Right limb diameter, mm	Left limb diameter, mm
EN1	25	16	16
EN2	25	16	16
EN3	28	16	16
EN4	25	20	16
EN5	28	20	16
EN6	32	20	20
EN7	25	20	20
EN8	25	20	16
EX1	23	16	16
EX2	28	16	16
EX3	23	14	14
EX4	28	14	14
EX5	28	14	16
EX6	23	20	16
EX7	23	16	16
EX8	26	14	16
AFX1	25	16	16
AFX2	28	16	16
AFX3	28	16	16
AFX4	28	16	20
AFX5	28	16	16
AFX6	25	16	16
AFX7	25	16	16
AFX8	28	16	16

EN = Endurant; EX = Excluder.

after EVAR for each patient. All patients were on optimal medical treatment (single antiplatelet agent, statins, and antihypertensive medication), and for this cohort of patients there was no event during the early post-operative period. Information about the CT system and the screening procedure can be found in our previous work where the same technique was employed.[26,27] The protocol was approved by the Institutional Review Board of the University of Ioannina, Greece and all subjects gave informed consent for the use of their data.

The endovascular devices under consideration were the ones that are mainly used in the study centre, so that several cases were accessible. Given that the effect of morphology on haemodynamics is prevalent, several cases are required to estimate the haemodynamic performance of a given endograft. The endografts included in the study represented a wide variety of design choices in terms of structure, material, and type of fixation. A brief analysis of their design is given below, while basic size characteristics of the stent graft systems used in each case are reported in Table 2.

AFX

The AFX Endovascular AAA System (Endologix) is a device designed to use the native aortic bifurcation to achieve fixation. The graft, composed of low porosity ePTFE, is attached to the exterior of the metallic cage with proximal and distal sutures. Consequently, the graft is allowed to move independently from the stent cage.[30]

Endurant. Endurant is a modular endovascular device composed of multifilament polyester fabric and electropolished Nitinol stents. Its suprarenal fixation system is made of a one piece Nitinol stent with anchoring pins while its first sealing stent is M shaped, providing neck conformability.[31]

Excluder. Excluder is a modular bifurcated stent graft composed of expanded polytetrafluoroethylene. It also includes a thin non-permeable layer of fluorinated ethylene propylene attached to its nitinol stent frame. The fixation of Excluder at the proximal neck is achieved at infrarenal level by the use of nitinol barbs.[30]

Nellix. Nellix consists of dual, balloon expandable, covered stents, each of which is surrounded by an endobag that is filled with an *in situ* curing polymer.[32] Each covered stent is surrounded by ePTFE and supports the blood flow lumen through the aneurysm sac to the iliac arteries without the need for proximal and distal fixation. The polymer containing endobags surround the flow lumen and fill the aneurysm sac providing anatomical fixation.[33]

Pre-operative morphological analysis

Initially, a pre-operative morphological analysis was carried out. Processing the pre-operative CT scans of the cases that

Table 3. Pre-operative abdominal aortic aneurysm morphological characteristics of the cases in each endograft group

	AFX	Endurant	Excluder	Nellix	*p*
Neck length, mm	27.6 ± 9.6	20.0 ± 6.0	26.6 ± 8.2	27.8 ± 11.7	0.19
Neck diameter, mm	23.2 ± 1.9	24.8 ± 3.1	22.6 ± 2.1	23.3 ± 2.6	0.25
Infrarenal angle, degrees	29.3 ± 12.5	21.4 ± 9.0	20.5 ± 13.6	25.7 ± 16.7	0.47
Suprarenal angle, degrees	20.4 ± 13.6	19.5 ± 10.0	16.9 ± 8.4	26.0 ± 13.8	0.41
Aorta length, mm	112.7 ± 16.6	105.9 ± 16.1	117.3 ± 9.3	115.6 ± 16.5	0.35
Right iliac length, mm	58.6 ± 9.6	65.9 ± 8.4	67.7 ± 16.9	65.6 ± 11.5	0.44
Right iliac diameter, mm	13.3 ± 1.7	15.5 ± 2.0	13.7 ± 2.0	13.8 ± 2.2	0.10
Neck to right iliac diameter	1.8 ± 0.3	1.6 ± 0.3	1.7 ± 0.2	1.7 ± 0.3	0.66
Left iliac length, mm	62.6 ± 7.3	70.2 ± 9.0	70.7 ± 14.7	62.2 ± 18.1	0.33
Left iliac diameter, mm	14.1 ± 2.0	14.4 ± 2.2	14 ± 2.7	13.2 ± 2.6	0.76
Neck to left iliac diameter	1.7 ± 0.3	1.7 ± 0.2	1.6 ± 0.2	1.8 ± 0.4	0.62

Values are given as means ± SDs.

met the inclusion criteria, the following morphological characteristics were extracted: neck length; neck diameter; suprarenal and infrarenal angle; aortic length; right and left iliac length; right and left iliac diameter; neck diameter to right iliac diameter; and neck diameter to left iliac diameter. All measurements were done with the medical imaging software 3mensio (Pie Medical Imaging BV, Maastricht, The Netherlands). The mean and standard deviation values of each morphological characteristic per endograft group are shown in Table 3. A one way ANOVA statistical test was performed for each morphological characteristic, concluding that the pre-operative morphology of the AAAs did not vary significantly between the endograft groups. The p values drawn from the statistical tests are shown in the last column of Table 3 and highlight the absence of statistically significant variation in the tested morhological characteristics.

Modelling

The computational workflow from CT scans to endograft specific haemodynamic indices is demonstrated in Fig. 1. The methodology involves the reconstruction of medical imaging data, 3D model refinement, computational mesh generation, CFD simulations, post-processing, and statistical analysis, all carried out in a range of commercial and open source software packages. Individual and paired haemodynamic analysis of the stent graft systems under consideration has been done previously by the present study group. Details about the steps of the methodology can be found in the relevant papers.[25–27]

Briefly, the methodology involves the reconstruction of the post-EVAR CT scans, focusing on the stented segment of the infrarenal abdominal aorta. The 3D post-operative lumen models include information about the post-implantation spatial configuration of the endografts. The surface of the models corresponds to the internal surface of the endograft device modelled as a rigid wall without thickness or material properties. A fluid structure interaction (FSI) approach is required to capture the interaction between blood flow and the device and access the stresses and strains experienced by the device. Using the triangulated surfaces, that are produced in the reconstruction phase, a CFD ready surface and volumetric computational mesh was generated, featuring high spatial resolution, sufficient to capture complex blood flow dynamics.[25–27]

Blood was modelled as a Newtonian fluid with density, $\rho = 1050\ kg/m^3$, and kinematic viscosity, $\nu = 3.2 \times 10^{-6}\ m^2/s$.[27] The no slip condition was imposed on the surface of the models according to the rigid wall assumption. A physiological pulse pressure condition was applied at the inlet and a physiological flow rate condition was applied at the outlets, based on Olufsen et al.[34]

Regions of interest

As a continuation of previous work, the present study is an assimilated analysis of the four stent graft systems, shifting the focus to specific areas in the implanted endovascular devices, above and beyond blood flow division. The regions of interest are sketched for indicative endograft cases in Fig. 2. The four endografts drive blood flow to the iliac arteries by different means. Endurant and Excluder are bifurcated proximally in the aneurysm sac, AFX uses the native abdominal aortic bifurcation, and Nellix is composed of two detached tubes that channel blood flow from the

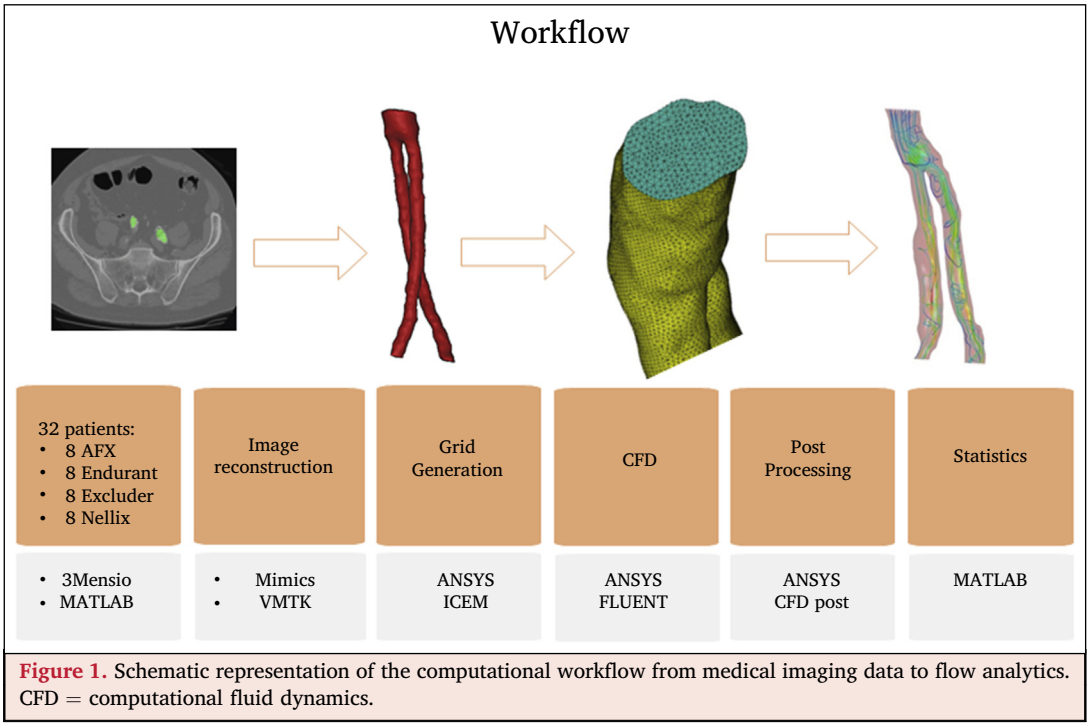

Figure 1. Schematic representation of the computational workflow from medical imaging data to flow analytics. CFD = computational fluid dynamics.

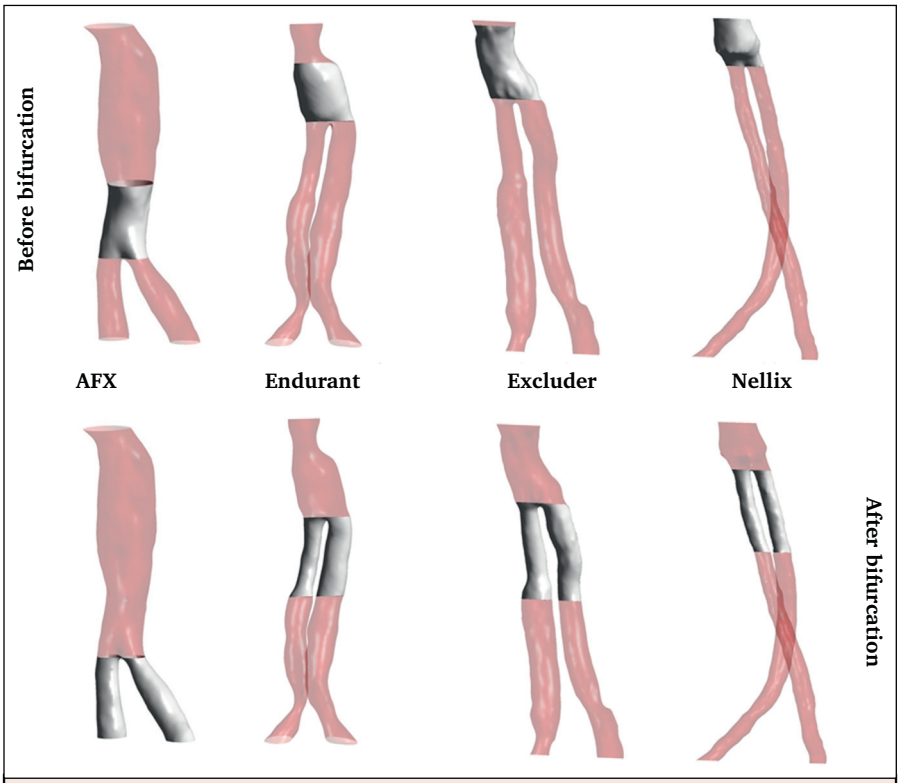

Figure 2. Regions of interest above and beyond the flow division sketched in representative endograft models of the four groups.

area immediately below the renal arteries all the way to the iliac arteries.

Haemodynamic properties

The haemodynamic properties used in the analysis were: velocity, WSS, and helicity. Specifically, the calculations were, i) the maximum velocity in the volume of the regions of interest at peak systole, ii) the maximum WSS on the surface of the regions of interest at peak systole, and iii) the mean helicity in the volume of the regions of interest at mid diastole.

Statistical analysis

Between and in group statistical analyses were performed using one way ANOVA and *t* tests, respectively. A value of $p < .05$ was considered to designate statistical significance. Furthermore, to identify possible correlation of hemodynamic parameters, the Pearson coefficient was calculated for the variables under consideration in both regions of interest (before and after bifurcation), using the software MATLAB (MathWorks Inc., Natick, Massachusetts, USA).

RESULTS

Velocity

As expected, the blood velocity is higher after the flow split, as blood flows in smaller diameters. According to the velocity chart in Fig. 3, the higher blood velocity, in both regions of interest, was recorded for Nellix cases, with statistically significant deviation from the AFX ($p = .03$), Endurant ($p < 0.001$), and Excluder ($p = .03$) cases, particularly in the region above the blood stream separation. Endurant, on the other hand, was associated with the lowest blood velocity among the endograft groups, both before and after the bifurcation. The mean value of maximum blood velocity was approximately equal in AFX and Excluder cases above the bifurcation, while after the flow separation, AFX induced the second highest velocity value with Excluder following in the third position.

WSS

Based on the corresponding chart in Fig. 3, the highest WSS value was found in the Nellix group, both above and beyond the bifurcation. There was a statistically significant difference between the Nellix and Endurant groups ($p = .03$) in terms of maximum WSS before blood flow separation. The lowest WSS value, as in the velocity measurements, was found in the Endurant cases, querying both regions of interest. The WSS findings in the AFX and Excluder groups followed the reverse trend compared with the velocity results. Specifically, maximum WSS before blood enters the limbs of AFX, was lower than the corresponding value in the Excluder group. In the upper segment of the limbs (directly after the endograft bifurcation), both endografts were associated with approximately equal WSS. The order of the endografts in terms of maximum WSS was: Nellix, in first

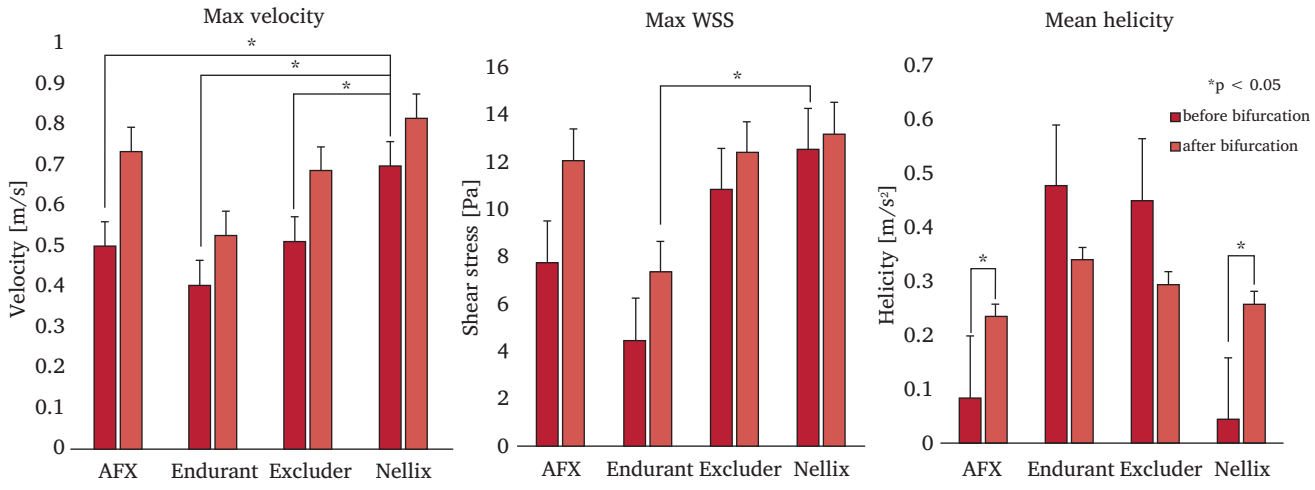

Before bifurcation

Variable	WSS_b	VEL_b	HELLI_b
WSS_b		r = .7153	r = .1088
		p < 0.001	p = .528
VEL_b	r = .7153		r = .0130
	p < 0.001		p = .940
HELLI_b	r = .1088	r = .0130	
	p = .528	p = .940	

After bifurcation

Variable	WSS_a	VEL_a	HELLI_a
WSS_a		r = .8903	r = .1546
		p < 0.001	p = .368
VEL_a	r = .8903		r = .0763
	p < 0.001		p = .658
HELLI_a	r = .1546	r = .0763	
	p = .368	p = .658	

Figure 3. Mean and SE values of the haemodynamic indices [velocity, wall shear stress (WSS), helicity] in both regions of interest in the four endograft groups. The asterisk indicates statistical significance. Below the charts, two tables with *r* and *p* values from the correlation analysis for the pairs of haemodynamics variables under consideration, where the indices "_b" and "_a" are attached to the variable names to indicate calculation before and after the bifurcation zone, respectively.

place, followed by AFX and Excluder, while the lowest values were attained in Endurant cases. Correlation analysis for all endografts showed that there was a strong correlation between maximum velocity and maximum WSS, both above and beyond the bifurcation, as expected, because local velocity and WSS are mathematically connected.

Helicity

The helicity results are presented in the last chart of Fig. 3. It is noted that AFX and Nellix follow a different trend from Endurant and Excluder. According to the measurements, AFX and Nellix exhibit higher mean helicity after the blood stream separation than before, while the reverse effect was evident in the other two endograft groups. Specifically, Endurant and Excluder were associated with high mean helicity values that drop after blood enters their limbs. The in-group variation of mean helicity between the 2 regions of interest was statically significant for the AFX ($p < 0.001$) and Nellix ($p < 0.001$) cases. In total, the highest helicity value, either before or after the bifurcation, was associated with the Endurant device, followed by Excluder, and Nellix and AFX which are very close in terms of helicity. A representation of the helical structures developing at several instances of the cardiac cycle, showing their dynamic evolution in indicative cases from each endograft group, is provided in Fig. 4. The differences in the quantitative helicity results are also apparent in the graphical representation of the helical structures.

DISCUSSION

Although the improved technical characteristics of the new generation EVAR devices addresses prior deficiencies, many challenges still exist.[35,36] Commercial endografts inherently differ in technical specifications and are associated with a variable frequency of post-operative adverse events, justifying the need for endograft specific analysis.[37,38] The computational approach has proven to be an effective way of exploring the impact of endograft implantation on blood flow, featuring significant benefits, such as non-invasiveness, low cost, high resolution analytics, and increased model customisability.

According to the results, the most statistically significant differences in velocity or WSS were found between Nellix and the remaining three endograft groups. The special design of Nellix, exploiting the endovascular sealing technology, seems to have an effect on blood flow. The device is composed of two separate tubes that are handling blood flow independently streaming it to the iliac arteries. It is computationally proven that Nellix induces the highest velocity and WSS (velocity gradient), which may be clinically translated as a reduced risk of in stent thrombogenicity given the absence of stagnant flow regions. It must also be noted that before blood flow splits to enter the Nellix limbs, the intensity of helical flow is reduced, which might be related to the fact that Nellix does not have a main body section compared with the remaining devices. According to the literature, blood flow

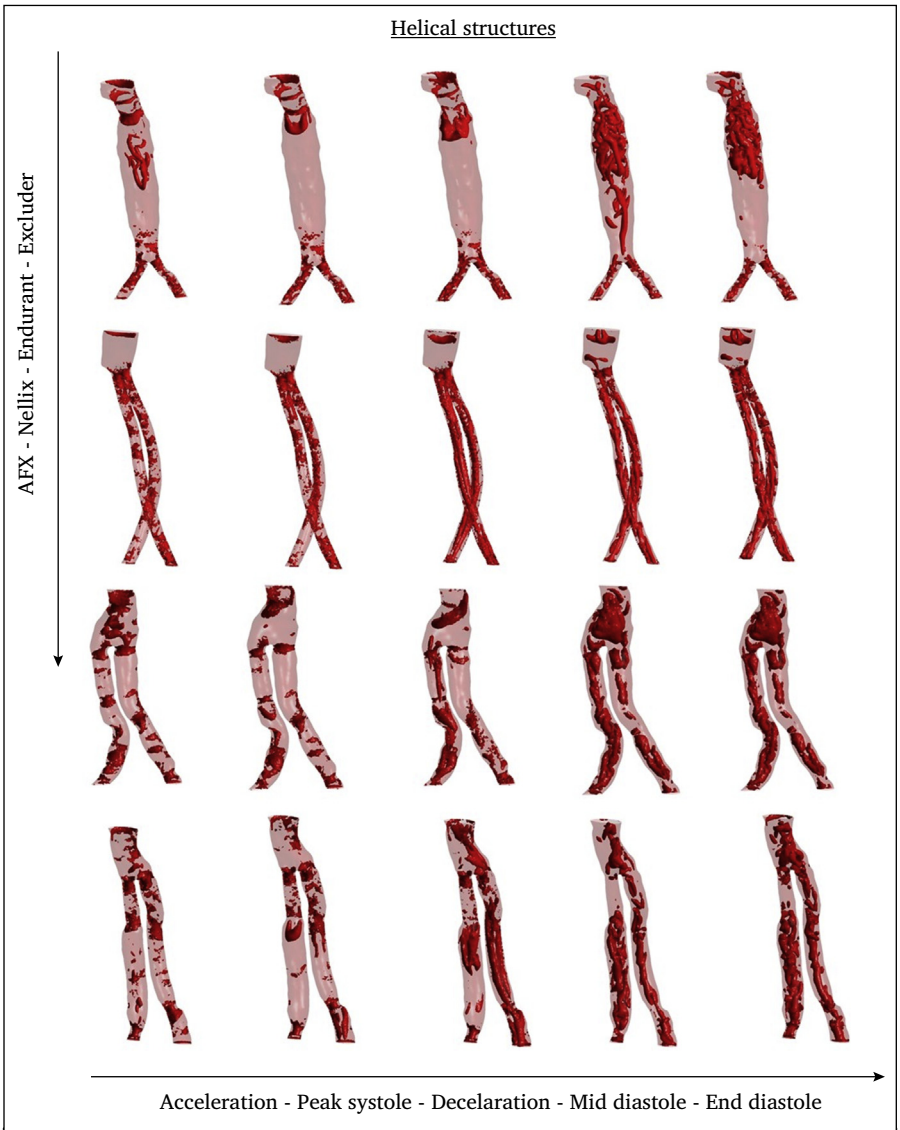

Figure 4. Demonstration of the helical structures developing at various points in the cardiac cycle, that is acceleration, peak systole, deceleration and mid-diastole phases, in representative cases from the four endograft groups.

near the renal arteries might be slightly altered by the deployment of a stent graft,[9] which, for the Nellix case, corresponds to the region before the flow division. In any case, there are no reports of any clinical implications deriving from the unique haemodynamic identity of Nellix so far.

On the other hand, Endurant and Excluder endografts which incorporate a main body section followed by a structured bifurcation high in the aneurysmal sac and two separate limbs, seem to preserve high intensity helicity before the flow division that diminishes downstream after the bifurcation. However, Endurant and Excluder endografts, despite the shared structure, induce distinct blood flow environments in terms of velocity and WSS that might be attributed to their dissimilar materials (polyester for the Endurant and ePTFE for the Excluder) and stent configuration.[26,28] Specifically, Endurant was associated with the lowest WSS values in the region around the bifurcation, which is in line with previous work by the present study group where regions of lower WSS were found to be larger in Endurant compared with Excluder or healthy cases.[27,28] Conversely the helicity results follow the same trend for both devices, probably attributed to their similar structure involving a short main body.

The AFX device has its main fixation point on the iliac bifurcation such that the post-EVAR lumen morphology resembles the physiological anatomy. Previous work has shown that AFX achieves restoration of blood flow indices to physiological levels. In the present study, AFX was associated with lower blood helicity values than Endurant and Excluder. It is of interest that there were similar results for the AFX and Nellix devices regarding helicity, both presenting low helicity before the bifurcation increasing afterwards, despite their dissimilar structure. Recently, it has

been suggested that the haemodynamic effects of the relative limb and in particular their lengths, should not be considered negligible. A high main body to iliac limb length ratio haemodynamically seems to favour a low bifurcation but it attenuates the main body iliac limbs modular stability.[22]

Recently, Boersen et al.[39] compared three endografts, Endurant, AFX, and Nellix, visualizing flow with laser particle imaging velocimetry. The endovascular aneurysm sealing (EVAS) experimental model, which is like a Nellix system, showed a stronger jet flow with a higher WSS rate in some regions compared with the other models. Small regions of low WSS and high oscillatory shear index were found near the distal end of all stents in the common iliac artery. They suggested that the different stent designs did not influence suprarenal flow. In the present study, comparing four stent graft systems, similar results were found with highest values of velocity and WSS being noted in the Nellix cases, despite not accounting for the suprarenal area. However, it is apparent that the flow profile is individualised for each device. Even, after the flow division, the trend of the results was preserved; Nellix induced the highest velocity and WSS, closely followed by Excluder and AFX.

Loss of limb patency varies between the endografts used in the present study, ranging from 3.4% for the Endurant to 1.1% for the Excluder.[40,41] In an experimental study, Demanget et al.[42] investigated the mechanical performance of eight different graft limbs. The authors concluded that spiral and circular stents may provide greater flexibility, as well as lower stress values, compared with Z stents. They further associated this with potentially better durability. These findings have been confirmed in the clinical setting in a retrospective study investigating the impact of stent grafting on aorto-iliac tortuosity. The reduction of the iliac tortuosity index was the least after Excluder implantation, probably as a result of better adaptation to the iliac anatomy.[43] Interestingly, no significant differences were found in graft limb complication rates between those stent grafts. More data are needed to affirm whether the differences in flow dynamics found in the present study, may be translated into different graft limb properties, which may eventually affect the clinical outcome.

Despite these differences between the endografts, clinical experience with all four devices has demonstrated good results at least during the early and mid term periods. The applicability of the Endurant stent graft has been thoroughly tested in several situations and showed promising results.[44] Additionally, the Excluder stent graft system with infrarenal fixation system has also yielded promising results.[45] EVAS with the use of Nellix has been suggested as a promising technique for treating AAA, and early efficacy data are encouraging in very suitable straightforward anatomy.[46] The real world use of the AFX endograft was associated with a low rate of device and procedure related complications.[47]

Studying the computational models of in stent flow may further assist in the evaluation of long term durability of endovascular devices and in further development of stent graft systems.[48] Specifically, a flow analysis inside endovascular devices could highlight undesired blood flow responses, which is clinically interpreted as creating an increased potential for complications. For instance, the existence of low WSS in parts of the endograft could lead to thrombus formation or limb occlusion according to the literature. As a result, it is suggested that endovascular devices should have a CFD evaluation in the context of clinical trials, driving the device design and adding a point of safety check carried out in computers non-invasively. To reveal the clinical impact of varying endograft based haemodynamics, long term follow up and larger case series may be needed. Future studies may use the current results to determine whether specific stent graft systems are more suitable for certain AAA anatomies with respect to parameters such as neck angulation, iliac bifurcation, endograft curvature, and length ratios, as well as iliac limb configuration.[49]

Limitations

The study relies on Newtonian modelling of blood flow while a non-Newtonian approach is considered to describe haemodynamics more accurately. However, according to the literature, the Newtonian model is sufficient for large arteries such as the abdominal aorta. As a pure CFD study, the thickness and material properties of the stent graft systems were not considered, which would require FSI modelling.[50] Nevertheless, a patient specific CFD analysis considers the real geometry of the lumen which mostly determines the haemodynamic conditions. The material properties of each device do not enter directly in the type of modelling applied in this study, but the elasticity (or rigidity) of the devices is reflected in the position and structure of the system in the aneurysmal region which is introduced in the models through reconstructions of the real patient medical imaging data. The rigid wall assumption is commonly used in endograft modelling when the velocity and shear stress fields or the displacement force from blood pressure are the crucial parameters in the study.[24,51] Because of the CFD type of modelling, the possible formation of biofilm that can occur inside endografts post-operatively is not taken into account.

Furthermore, the measurements presented in the current study do not correspond to or predict clinical events. Longer follow up and a larger number of patients are needed to further describe the haemodynamic performance and the flow characteristics of the various endovascular devices. Future studies considering longer term follow up may be needed to examine in more depth the association between flow disturbances and clinical events. Furthermore, selection of the devices for inclusion in the study was based on these four types of stent graft systems being most commonly used at the study centre, and thus being more accessible. In this respect, bias from the endograft selection

may be present. In any case, the endografts studied here represent a wide variety of design choices regarding material, structure, type of fixation, and other technical specifications.

CONCLUSIONS

The current study deals with the post-EVAR flow conditions in four stent graft systems with different designs, materials, and types of fixation. Using computational fluid dynamics software simulations, it was shown that endografts with different anatomical characteristics demonstrated different haemodynamic parameters. There were differences in the haemodynamic conditions in the area near the flow divider depending on the endograft type, while differences in the flow conditions of several different limb configurations were also noted. Future studies are needed to examine whether these differences in haemodynamic characteristics may have a clinical impact in the long term follow up of the patients. The study suggests that computational assessment of the quality of post-EVAR blood flow should be extended in all devices, as represented by larger patient cohorts.

CONFLICT OF INTEREST

None.

FUNDING

None.

REFERENCES

1 Dangas G, O'Connor D, Firwana B, Brar S, Ellozy S, Vouyouka A, et al. Open versus endovascular stent graft repair of abdominal aortic aneurysms: a meta-analysis of randomized trials. *JACC Cardiovasc Interv* 2012;**5**:1071–80.
2 Stather PW, Sidloff D, Dattani N, Choke E, Bown MJ, Sayers RD. Systematic review and meta-analysis of the early and late outcomes of open and endovascular repair of abdominal aortic aneurysm. *Br J Surg* 2013;**100**:863–72.
3 IMPROVE Trial Investigators. Endovascular strategy or open repair for ruptured abdominal aortic aneurysm: one-year outcomes from the IMPROVE randomized trial. *Eur Heart J* 2015;**36**:2061–9.
4 Tadros RO, Faries PL, Ellozy SH, Lookstein RA, Vouyouka AG, Schrier R, et al. The impact of stent graft evolution on the results of endovascular abdominal aortic aneurysm repair. *J Vasc Surg* 2014;**59**:1518–27.
5 Al-Jubouri M, Comerota AJ, Thakur S, Aziz F, Wanjiku S, Paolini D, et al. Reintervention after EVAR and open surgical repair of AAA: a 15-year experience. *Ann Surg* 2013;**258**:652–7.
6 Li Z, Kleinstreuer C, Farber M. Computational analysis of biomechanical contributors to possible endovascular graft failure. *Biomech Model Mechan* 2005;**4**:221–34.
7 Molony DS, Callanan A, Kavanagh EG, Walsh MT, McGloughlin TM. Fluid-structure interaction of a patient-specific abdominal aortic aneurysm treated with an endovascular stent-graft. *Biomed Eng Online* 2009;**8**:12.
8 Argani L, Torella F, Fisher R, McWilliams R, Wall M, Movchan A. Deformation and dynamic response of abdominal aortic aneurysm sealing. *Sci Rep* 2017;**7**:17712.
9 Walsh PW, Chin-Quee S, Moore JE. Flow changes in the aorta associated with the deployment of a AAA stent graft. *Med Eng Phys* 2003;**25**:299–307.
10 Vardoulis O, Coppens E, Martin B, Reymond P, Tozzi P, Stergiopulos N. Impact of aortic grafts on arterial pressure: a computational fluid dynamics study. *Eur J Vasc Endovasc Surg* 2011;**42**:704–10.
11 Maleux G, Koolen M, Heye S. Complications after endovascular aneurysm repair. *Semin Intervent Rad* 2009;**26**:3–9.
12 Shek TL, Tse LW, Nabovati A, Amon CH. Computational fluid dynamics evaluation of the cross-limb stent graft configuration for endovascular aneurysm repair. *J Biomech Eng* 2012;**134**:121002.
13 Chaikof EL, Dalman RL, Eskandari MK, Jackson BM, Lee WA, Mansour MA, et al. The Society for Vascular Surgery practice guidelines on the care of patients with an abdominal aortic aneurysm. *J Vasc Surg* 2018;**67**:2–77.
14 Wu I, Liang P, Huang S, Chi N, Lin F, Wang S. The significance of endograft geometry on the incidence of intraprosthetic thrombus deposits after abdominal endovascular grafting. *Eur J Vasc Endovasc Surg* 2009;**38**:741–7.
15 Mestres G, Maeso J, Fernandez V, Allegue N, Constenla I, Matas M. Incidence and evolution of mural thrombus in abdominal aortic endografts. *Ann Vasc Surg* 2009;**23**:627–33.
16 Wegener M, Görich J, Krãmer S, Fleiter T, Tomczak R, Scharrer-Pamler R, et al. Thrombus formation in aortic endografts. *J Endovasc Ther* 2001;**8**:372–9.
17 Maleux G, Koolen M, Heye S, Heremans B, Nevelsteen A. Mural thrombotic deposits in abdominal aortic endografts are common and do not require additional treatment at short-term and midterm follow-up. *J Vasc Interv Radiol* 2008;**19**:1558–62.
18 Lowe GD. Virchow's triad revisited: abnormal flow. *Pathophysiol Haemost Thromb* 2003;**33**:455–7.
19 Yeow SL, Leo HL. Hemodynamic study of flow remodeling stent graft for the treatment of highly angulated abdominal aortic aneurysm. *Comput Math Methods Med* 2016;**2016**:3830123.
20 Polanczyk A, Piechota-Polanczyk A, Stefanczyk L. A new approach for the pre-clinical optimization of a spatial configuration of bifurcated endovascular prosthesis placed in abdominal aortic aneurysms. *PLoS One* 2017;**12**:e0182717.
21 Polanczyk A, Podyma M, Trebinski L, Chrzastek J, Zbicinski I, Stefanczyk L. A novel attempt to standardize results of CFD simulations basing on spatial configuration of aortic stent-grafts. *PLoS One* 2016;**11**.
22 Molony DS, Callanan A, Morris LG, Doyle BJ, Walsh MT, McGloughlin TM. Geometrical enhancements for abdominal aortic stent-grafts. *J Endovasc Ther* 2008;**15**:518–29.
23 Casciaro M, Alfonso M, Craiem D, Alsac J, El-Batti S, Armentano R. Predicting the effect on pulse wave reflection of different endovascular repair techniques in abdominal aortic aneurysm using 1D patient-specific models. *Health Technol* 2016;**6**:173–9.
24 Aristokleous N, Kontopodis NG, Tzirakis K, Ioannou CV, Papaharilaou Y. Hemodynamic impact of abdominal aortic aneurysm stent-graft implantation-induced stenosis. *Med Biol Eng Comput* 2016;**54**:1523–32.
25 Raptis A, Xenos M, Kouvelos G, Giannoukas A, Matsagkas M. Haemodynamic performance of AFX and Nellix endografts: a computational fluid dynamics study. *Interact Cardiovasc Thorac Surg* 2018;**26**:826–33.
26 Raptis A, Xenos M, Georgakarakos E, Kouvelos G, Giannoukas A, Matsagkas M. Hemodynamic profile of two aortic endografts accounting for their postimplantation position. *J Med Device* 2017;**11**:021003.
27 Raptis A, Xenos M, Georgakarakos E, Kouvelos G, Giannoukas A, Labropoulos N, et al. Comparison of physiological and post-endovascular aneurysm repair infrarenal blood flow. *Comput Methods Biomec* 2016:1–8.
28 Tasso P, Raptis A, Matsagkas M, Lodi Rizzini M, Gallo D, Xenos M, et al. Abdominal aortic aneurysm endovascular repair: profiling post-implantation morphometry and hemodynamics with image-

based computational fluid dynamics. *J Biomech Eng* 2018. https://doi.org/10.1115/1.4040337 [Epub ahead of print].
29 Perrin D, Badel P, Orgéas L, Geindreau C, Dumenil A, Albertini J-N, et al. Patient-specific numerical simulation of stent-graft deployment: validation on three clinical cases. *J Biomech* 2015;**48**:1868–75.
30 Eckroth-Bernard K, Garvin R, Ryer E. Current status of endovascular devices to treat abdominal aortic aneurysms. *Biomed Eng Comput Biol* 2013;**5**:25–32.
31 Makaroun MS, Tuchek M, Massop D, Henretta J, Rhee R, Buckley C, et al. One year outcomes of the United States regulatory trial of the endurant stent graft system. *J Vasc Surg* 2011;**54**:601–8.
32 Buck DB, van Herwaarden JA, Schermerhom ML, Moll FL. Endovascular treatment of abdominal aortic aneurysms. *Nat Rev Cardiol* 2014;**11**:112–23.
33 Krievins DK, Holden A, Savlovskis J, Calderas C, Donayre CE, Moll FL, et al. EVAR using the Nellix sac-anchoring endoprosthesis: treatment of favourable and adverse anatomy. *Eur J Vasc Endovasc Surg* 2011;**42**:38–46.
34 Olufsen MS, Peskin CS, Kim WY, Pedersen EM, Nadim A, Larsen J. Numerical simulation and experimental validation of blood flow in arteries with structured-tree outflow conditions. *Ann Biomed Eng* 2000;**28**:1281–99.
35 Desai M, Eaton-Evans J, Hillery C, Bakhshi R, You Z, Lu J, et al. AAA stent-grafts: past problems and future prospects. *Ann Biomed Eng* 2010;**38**:1259–75.
36 Corbett TJ, Callanan A, Morris LG, Doyle BJ, Grace PA, Kavanagh EG, et al. A review of the in vivo and in vitro biomechanical behavior and performance of postoperative abdominal aortic aneurysms and implanted stent-grafts. *J Endovasc Ther* 2008;**15**:468–84.
37 Propper BW, Abularrage CJ. Long-term safety and efficacy of endovascular abdominal aortic aneurysm repair. *Vasc Health Risk Manag* 2013;**9**:135–41.
38 Van Marrewijk CJ, Leurs LJ, Vallabhaneni SR, Harris PL, Buth J, Laheij RJF. Risk-adjusted outcome analysis of endovascular abdominal aortic aneurysm repair in a large population: how do stent-grafts compare? *J Endovasc Ther* 2005;**12**:417–29.
39 Boersen JT, Groot Jebbink E, Versluis M, Slump CH, Ku DN, de Vries JPM, et al. Flow and wall shear stress characterization after endovascular aneurysm repair and endovascular aneurysm sealing in an infrarenal aneurysm model. *J Vasc Surg* 2017;**66**:1844–53.
40 Pratesi C, Piffaretti G, Pratesi G, Castelli P, ITalian Excluder Registry Investigators. Italian Excluder Registry and results of Gore Excluder endograft for the treatment of elective infrarenal abdominal aortic aneurysms. *J Vasc Surg* 2014;**59**:52–7.
41 Faure EM, Becquemin J-P, Cochennec F, Monaco RG, Ferreira M, Fitridge R, et al. Predictive factors for limb occlusions after endovascular aneurysm repair. *J Vasc Surg* 2015;**61**:1138–45.e1132.
42 Demanget N, Duprey A, Badel P, Orgeas L, Avril S, Geindreau C, et al. Finite element analysis of the mechanical performances of 8 marketed aortic stent-grafts. *J Endovasc Ther* 2013;**20**:523–35.
43 Coulston J, Baigent A, Selvachandran H, Jones S, Torella F, Fisher R. The impact of endovascular aneurysm repair on aortoiliac tortuosity and its use as a predictor of iliac limb complications. *J Vasc Surg* 2014;**60**:585–9.
44 Deery SE, Shean KE, Pothof AB, O'Donnell TFX, Dalebout BA, Darling JD, et al. Three-year results of the Endurant stent graft system post approval study. *Ann Vasc Surg* 2018;**50**:202–8.
45 Krajcer Z. The Gore Excluder AAA endoprosthesis with C3 delivery system: results in high-volume centers. *J Cardiovasc Surg (Torino)* 2014;**55**:41–9.
46 Unlu C, Schuurmann RCL, de Vries J. The Nellix device: review of indications and outcome. *Expert Rev Med Dev* 2017;**14**:651–6.
47 Welborn MB, McDaniel HB, Johnson RC, Kennedy RE, Knott A, Mundinger GH, et al. Clinical outcome of an extended proximal seal zone with the AFX endovascular aortic aneurysm system. *J Vasc Surg* 2014;**60**:876–83.
48 Zarins CK, Taylor CA. Endovascular device design in the future: transformation from trial and error to computational design. *J Endovasc Ther* 2009;**16**:12–21.
49 Georgakarakos E, Argyriou C, Schoretsanitis N, Ioannou CV, Kontopodis N, Morgan R, et al. Geometrical factors influencing the hemodynamic behavior of the AAA stent grafts: essentials for the clinician. *Cardiovasc Intervent Radiol* 2014;**37**:1420–9.
50 Prasad A, Xiao N, Gong XY, Zarins CK, Figueroa CA. A computational framework for investigating the positional stability of aortic endografts. *Biomech Model Mechan* 2013;**12**:869–87.
51 Stefanov F, McGloughlin T, Morris L. A computational assessment of the hemodynamic effects of crossed and non-crossed bifurcated stent-graft devices for the treatment of abdominal aortic aneurysms. *Med Eng Phys* 2016;**38**:1458–73.